Inorg. Chem. **2007**, *46*, 3680–3687

Thermodynamics and Kinetics of the Nickel(II)–Salicylhydroxamic Acid System. Phenol Rotation Induced by Metal Ion Binding

Begoña García,*,† Sheila Gonzalez,† Francisco J. Hoyuelos,† Saturnino Ibeas,† José M. Leal,† María L. Senent,‡ Tarita Biver,§ Fernando Secco,*,§ and Marcella Venturini§

Departamento de Química, Universidad de Burgos, 09001 Burgos, Spain, Departamento de Astrofísica Molecular e Infrarroja, Instituto de Estructura de la Materia, Consejo Superior de Investigaciones Cientificas, 28006 Madrid, Spain, and Dipartimento di Chimica e Chimica Industriale, Università di Pisa, 56126 Pisa, Italy

Received July 27, 2006

The kinetics and the equilibria of Ni(II) binding to *p*-hydroxybenzohydroxamic acid (PHBHA) and salicylhydroxamic acid (SHA) have been investigated in an aqueous solution at 25 °C and $I = 0.2$ M by the stopped-flow method. Two reaction paths involving metal binding to the neutral acid and to its anion have been observed. Concerning PHBHA, the rate constants of the forward and reverse steps are $k_1 = (1.9 \pm 0.1) \times 10^3$ M^{-1} s^{-1} and $k_{-1} = (1.1 \pm 0.1) \times 10^2$ s^{-1} for the step involving the undissociated PHBHA and $k_2 = (3.2 \pm 0.2) \times 10^4$ M^{-1} s^{-1} and $k_{-2} = 1.2 \pm 0.2$ s^{-1} for the step involving the anion. Concerning SHA, the analogous rate constants are $k_1 = (2.6 \pm 0.1) \times 10^3$ M^{-1} s^{-1}, $k_{-1} = (1.3 \pm 0.1) \times 10^3$ s^{-1}, $k_2 = (5.4 \pm 0.2) \times 10^3$ M^{-1} s^{-1}, and $k_{-2} = 6.3 \pm 0.5$ s^{-1}. These values indicate that metal binding to the anions of the two acids concurs with the Eigen–Wilkins mechanism and that the phenol oxygen is not involved in the chelation. Moreover, a slow effect was observed in the SHA–Ni(II) system, which has been put down to rotation of the benzene ring around the C–C bond. Quantum mechanical calculations at the B3LYP/lanL2DZ level reveal that the phenol group in the most stable form of the Ni(II) chelate is in trans position relative to the carbonyl oxygen, contrary to the free SHA structure, where the phenol and carbonyl oxygen atoms both have cis configuration. These results bear out the idea that the complex formation is coupled with phenol rotation around the C–C bond.

Introduction

Hydroxamic acids, RCONR′OH, have been known for a long time.[1]However, their importance has been fully recognized only in the last 20 years, after a large amount of information had been accumulated on their chemical role as efficient binding ligands for metal ions with industrial, environmental, and medicinal applications. The hydroxamate group, a constituent of the siderophores, the naturally occurring iron(III) carriers, also plays an important role in biology.[2,3] A comprehensive review of the solution and structural chemistry and biological function of siderophores and their metal complexes, whose ligand protonation and complex formation constants are reported, has been published by Raymond et al.[44] More recently, hydroxamic acids have received renewed interest due to their use as effective inhibitors of enzymes[5,6] and as potential drugs for the treatment of a variety of diseases on account of their hypotensive,[7] anticancer,[8−12] antimalarial,[13−17] and antifungal[18] properties.

* To whom correspondence should be addressed. E-mail: ferdi@dcci.unipi.it (F.S.), begar@ubu.es (B.G.).
† Universidad de Burgos.
‡ Consejo Superior de investigaciones Cientificas de Madrid.
§ Università di Pisa.

(1) Lossen, H. *Liebigs Ann. Chem.* **1869**, *150*, 314−320.
(2) Winkelmann, G.; Van der Helm, D.; Nielands, J. B. *Iron Transport in Microbes, Plants and Animals*; VCH: New York, 1987.
(3) Albrecht-Gary, A. M.; Crumbliss, A. L. In *Metal Ions in Biological Systems*; Sighel, A., Sighel, H., Eds.; Marcel Dekker: New York, 1998; Vol. 35, p 239.
(4) Raymond, N. K.; Mueller, G.; Matzanke, B. F. *Top. Curr. Chem.* **1984**, *123*, 49−102.
(5) Muri, E. M.; Nieto, M. J.; Sindelar, R. D.; Williamson, J. S. *Curr. Med. Chem.* **2000**, *7*, 1631−1653.
(6) Lou, B.; Yang, K. *Mini−Rev. Med. Chem.* **2003**, *3*, 609−620.
(7) Zamora, R.; Grzesiok, A.; Weber, H.; Feelisch, M. *Biochem. J.* **1995**, *312 (Part 2)*, 333−339.
(8) Steward, W. P.; Thomas, A. L. *Expert Opin. Invest. Drugs* **2000**, *9*, 2913−2922.
(9) Bouchain, G.; Delorme, D. *Curr. Med. Chem.* **2003**, *10*, 2359−2372.
(10) Steward, W. P. *Cancer Chemother. Pharmacol.* **1999**, *43 Suppl*, S 56−60.

10.1021/ic0614061 CCC: $37.00
Published on Web 04/06/2007

Salicylhydroxamic acid (SHA), with a phenol group ortho to the hydroxamic group, offers additional geometry and ligand possibilities compared with the parent and simpler benzohydroxamic acid (BHA) and even with the *p*-hydroxybenzohydroxamic acid (PHBHA) isomer. In addition to the well-known E/Z and amide/imide equilibria displayed by simple hydroxamic acids, some other different, stable SHA structures are also feasible for rotation around the C−C bond, as shown below; if A and B stand for two different conformer

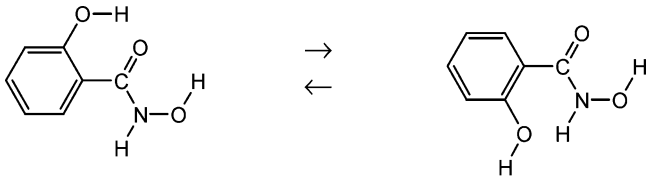

A B

families generated according to such a rotation, then it can be inferred that the A conformer would result in a more stable structure than conformer B; that is because the formation of a hydrogen bond between the phenol hydrogen and the carbonyl oxygen is feasible in A, whereas it is unfeasible in B. Indeed, a recent study of the SHA structure in the gas phase and in DMSO shows that structure A is the most stable.[19] This result suggests that in aprotic solvents form A is far more prevalent; however, it is expected that in water the intramolecular hydrogen bonds will become weakened, thus bringing about a lowering of the molecular rigidity.

Concerning the binding of metal ions to hydroxamic acids, it should be noted that metal chelation involves binding to the carbonyl (O_C) and hydroxamate (O_H) oxygen atoms (with concomitant ligand deprotonation). In the A conformation, chelation for SHA comes about at the carbonyl and phenol (O_P) oxygen atoms, as was already found for the SHA−Pt(II) system.[20,21] More interestingly, a $Pd(SHA)_2$ complex has been synthesized whose crystal structure reveals a [NO_P] binding mode.[22] The B form of SHA presents two sites which, in principle, could bind a metal ion. One of them is the usual O_C O_H site, whereas the other is the O_P N site. Metal complexation at both SHA sites is observed in metallacrowns, as the macrocyclic structures are able to selectively encapsulate cations or anions. Metallacrowns were put forward for the first time by Pecoraro and his school;[23−25] these authors widely employed SHA to synthesize metallacrowns containing Mn(III), Fe(III), V(V), Cu(II), and Ni(II) in the macrocyclic ring. The SHA-based metallacrowns are stable in DMSO, in dry DMF, and, to some extent, in methanol but not in water.[26] Subsequent to such a discovery, various research groups have been engaged in the synthesis and characterization of metallacrowns based mainly on aminohydroxamate ligands, which appear to be stable in aqueous solutions.[27,28]

We present here a study on the equilibria and the kinetics of binding of the Ni^{2+} ion to both SHA and its PHBHA isomer along with theoretical calculations of the energies of the Ni(II) complexes with the A and B SHA isomers. This study has been performed to obtain a picture of the eventual conformation changes coupled with the complex formation, to find the preferred reaction site, and to elucidate the mechanism of the metal−ligand interaction.

Experimental and Computational Section

Materials. All chemicals were analytical grade (Fluka or Aldrich). The SHA and PHBHA solutions were prepared by weighing the appropriate amounts of solid reagent (purity >99%) and dissolving them in water. The concentrations of Ni(II) and Zn(II), present as perchlorate in the stock solutions, were measured by EDTA titrations.[29] Sodium perchlorate was used to attain the desired ionic strength. To keep the pH constant, cacodylic acid ($(CH_3)_2As(O)OH$, $pK_a = 6.19$)[30] partly neutralized with NaOH was used. Doubly deionized water from a Millipore Q apparatus (APS; Los Angeles, CA) was used in the preparation of the solutions and as a reaction medium.

Methods. The hydrogen ion concentration of the aqueous solutions was measured by a Metrohm 713 pH meter. The instrument output was converted to hydrogen ion concentration by the relationship $[H^+] = 10\ \exp(0.13 - pH)$, which was obtained by a suitable calibration procedure.[30] The absorption spectra were recorded on Perkin-Elmer Lambda 35 and HP B453 (diode array) spectrophotometers. The titrations were performed by syringing increasing micro amounts of the metal ion solution to a ligand solution (SHA or PHBHA) already thermostatted in the measuring cell. All measurements were performed under a nitrogen atmosphere.

(11) Brammer, R.; Buckels, J.; Bramhall, S. *Int. J. Clin. Pract.* **2000**, *54*, 373−381.
(12) Holms, J.; Mast, K.; Marcotte, P.; Elmore, I.; Li, J.; Pease, L.; Glaser, K.; Morgan, D.; Michaelides, M.; Davidsen, S. *Bioorg. Med. Chem. Lett.* **2001**, *11*, 2907−2910.
(13) Mishra, R. C.; Tripathi, R.; Katiyar, D.; Tewari, N.; Singh, D.; Tripathi, R. P. *Bioorg. Med. Chem.* **2003**, *11*, 5363−5674.
(14) Apfel, C.; Banner, D. W.; Bur, D.; Dietz, M.; Hirata, T.; Hubschwerlen, C.; Locher, H.; Page, M. G. P.; Pirson, W.; Rosse, G.; Specklin, J. L. *J. Med. Chem.* **2000**, *43*, 2324−2331.
(15) Holland, K. P.; Elford, H. L.; Bracchi, V.; Annis, C. G.; Schuster, S. M.; Chakrabarti, D. *Antimicrob. Agent Chemother.* **1998**, *42*, 2456−2458.
(16) Tsafack, A.; Golenser, J. J.; Libman, J.; Shanzer, A.; Cabantchik, Z. I. *Antimicrob. Agent Chemother.* **1995**, *47*, 403−409.
(17) Golenser, J.; Tsafack, A.; Amichai, Y.; Libman, J.; Shanzer, A.; Cabantchik, Z. I. *Antimicrob. Agent Chemother.* **1995**, *39*, 61−65.
(18) Miller, M. J. *Chem. Rev.* **1989**, *89*, 1563−1579 and references cited therein.
(19) Kaczor, A.; Szczepanski, J.; Vala, M.; Proniewicz, L. M. *Phys. Chem. Chem. Phys.* **2005**, *7*, 1960−1965.
(20) Hall, M. D.; Failes, T. W.; Hibbs, D. E.; Hambley, T. W. *Inorg. Chem.* **2002**, *41*, 1223−1228.
(21) Henderson, W.; Evans, C.; Nicholson, B. K.; Facwcett, J. *Dalton Trans.* **2003**, 2691−2697.
(22) Hall, M. D.; Failes, T. W.; Hibbs, D. E.; Hambley, T. W. *Inorg. Chem.* **2002**, *41*, 1223−1228.
(23) Lah, M. S; Kirk, M. L.; Hatfield, W.; Pecoraro, V. L. *J. Chem. Soc., Chem. Commun.* **1989**, 1606−1608.
(24) Lah, M. S; Pecoraro, V. L. *Comments Inorg. Chem.* **1990**, *11*, 59−84.
(25) Pecoraro, V. L. *Inorg. Chim. Acta* **1989**, *155*, 171−173.
(26) Pecoraro, V. L.; Stemmler, A. J.; Gibney, B. R.; Bodwin, J. J.; Wang, H.; Kampf, J. W.; Barwinski, A. In *Progress in Inorganic Chemistry*; Karlin, K. D., Ed.; Wiley: New York, 1997; Vol. 45, pp 83−177.
(27) Kurzak, B.; Farkas, E.; Glowiak, T.; Kozlowski, H. *J. Chem. Soc., Dalton Trans.* **1991**, 163−167.
(28) Tegoni, M.; Dallavalle, F.; Belosi, B.; Remelli, M. *Dalton Trans.* **2004**, 1329−1333.
(29) Orrichi, H. In *Treatise of Analytical Chemistry*; Kolthoff, I. M., Helving, O. J., Eds.; Interscience: New York, 1962; Part II, Vol. 2.
(30) Diebler, H.; Secco, F.; Venturini, M. *J. Phys. Chem.* **1984**, *33*, 4229−4232.

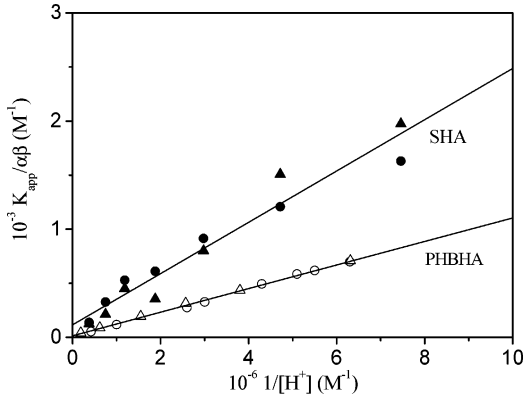

Figure 1. Dependence of the apparent Ni(II)−ligand binding constants on the reciprocal H ion concentration for the investigated hydroxamic acids at 25 °C and $I = 0.2$ M. Symbols: triangles, thermodynamic data; circles, kinetic data. The intercept (b) and slope (m) values for PHBHA are $b = 14.8$ M^{-1} and $m = 1.09 \times 10^{-4}$, which give $K_{MH_2L} = 14.8$ M^{-1} and $K_{MHL} = 2.74 \times 10^4$ M^{-1}; values for SHA are $b = 1.15 \times 10^2$ M^{-1} and $m = 2.37 \times 10^{-4}$, which give $K_{MH_2L} = 1.15 \times 10^2$ M^{-1} and $K_{MHL} = 4.95 \times 10^3$ M^{-1}.

The kinetic experiments concerning the SHA complex formation with Ni(II) and Zn(II) were all performed on a Biologic SFM 300 stopped-flow mixing unit coupled to a spectrophotometric line by two optical guides. The UV radiation from a Hamamatsu L248102 "quiet" lamp was passed through a Baush and Lomb 338875 high-intensity monochromator and then split into two beams. The reference beam was sent directly to a 1P28 photomultiplier. The output from the two photomultipliers was balanced before each shot. The acquisition system keeps a record of a number of data points ranging from 10 to 8000 with a sampling interval in the 50 μs to 10 s time scale. The kinetics of the PHBHA−Ni(II) system were investigated with a Biologic SFM 400 instrument.

Theoretical Calculations. Geometry optimization of the SHA−Ni(II) system in the gas phase has been achieved using the *Gaussian 03* package of programs.[31] The calculations have been started at the HF/LanL2DZ level and then refined with density functional theory (calculation B3LYP/LanL2DZ).[32−35] Calculations for the Ni(II)−SHA·$2H_2O$ (A and B) and Ni(II)−PHBHA·$2H_2O$ complexes were performed with the LanL2DZ basis set containing the effective core potential from the Los Alamos group.[33−35]

Results

Equilibria. The equilibria of the interactions of PHBHA and SHA with Ni^{2+} ions in an aqueous solution have been investigated by spectrophotometric titrations in the 5.5−7.4 pH range; below pH 5.5, the extent of binding was too limited to be reliably evaluated, whereas above pH 7.4, precipitation of $Ni(OH)_2$ has been observed. All equilibrium (and kinetic) measurements were performed under metal excess to ensure that only 1:1 complexes were formed. Figure 1SA (Supporting Information) shows the spectra of PHBHA recorded (a) in the absence and (b) in the presence of $Ni(ClO_4)_2$. The analogous spectra for SHA are shown in Figure 1SB (Supporting Information). The titrations were performed at $\lambda = 288$ nm for PHBHA and at $\lambda = 268$ and 304 nm for SHA. During the titration, the solution pH was kept constant at the desired value by a buffer made of 3×10^{-3} M cacodylic acid partially neutralized with NaOH. This buffer does not bind to the Ni^{2+} ion.[36] Under these circumstances, the equilibria could be described by the apparent reaction 1

$$M_f + L_f \rightleftharpoons ML_T \quad (1)$$

where $M_f = [M^{2+}]$, $L_f = [H_2L] + [HL^-]$, and $ML_T = [MH_2L^{2+}] + [MHL^+]$. Other species such as MOH^+, L^{2-}, and ML have not been considered since, in the investigated pH range, their amounts are negligible. The equilibrium constant of reaction 1, K_{app}, was evaluated at different pH values by analyzing the spectral changes according to a procedure previously described,[37] which leads to plots like that shown in Figure 2S (Supporting Information); the values for PHBHA and SHA are collected in Tables 1S and 2S, respectively (Supporting Information). The K_{app} values were found to depend on $[H^+]^{-1}$ according to eq 2

$$K_{app}/\alpha\beta = K_{MH_2L} + K_{H_2L}K_{MHL}/[H^+] \quad (2)$$

where $\alpha = [H^+]/([H^+] + K_{H_2L})$ and $\beta = [M^{2+}]/[M_f] \approx 1$ over the investigated range of $[H^+]$. Equation 2 has been derived on the basis of the reactions shown in Scheme 1.

Scheme 1

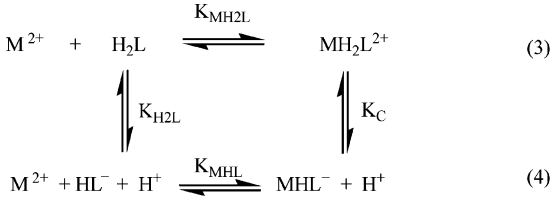

The equilibrium data, plotted in Figure 1 according to eq 2, yielded the values of the individual equilibrium constants, K_{MH_2L} and K_{MHL}, which are collected in Table 1 together with the values of the independently determined acid dissociation constants.[38]

Kinetics. The kinetics of complex formation have been investigated by the stopped-flow method under pseudo-first-

(31) Frisch, M. J.; Trucks, G. W.; Schlegel, H. B.; Scuseria, G. E.; Robb, M. A.; Cheeseman, J. R.; Montgomery, J. A. Jr.; Vreven, T.; Kudin, K. N.; Burant, J. C.; Millam, J. M.; Iyengar, S. S.; Tomasi, J.; Barone, V.; Mennucci, B.; Cossi, M.; Scalmani, G.; Rega, N.; Petersson, G. A.; Nakatsuji, H.; Hada, M.; Ehara, M.; Toyota, K.; Fukuda, R.; Hasegawa, J.; Ishida, M.; Nakajima, T.; Honda, Y.; Kitao, O.; Nakai, H.; Klene, M.; Li, X.; Knox, J. E.; Hratchian, H. P.; Cross, J. B.; Bakken, V.; Adamo, C.; Jaramillo, J.; Gomperts, R.; Stratmann, R. E.; Yazyev, O.; Austin, A. J.; Cammi, R.; Pomelli, C.; Ochterski, J. W.; Ayala, P. Y.; Morokuma, K.; Voth, G. A.; Salvador, P.; Dannenberg, J. J.; Zakrzewski, V. G.; Dapprich, S.; Daniels, A. D.; Strain, M. C.; Farkas, O.; Malick, D. K.; Rabuck, A. D.; Raghavachari, K.; Foresman, J. B.; Ortiz, J. V.; Cui, Q.; Baboul, A. G.; Clifford, S.; Cioslowski, J.; Stefanov, B. B.; Liu, G.; Liashenko, A.; Piskorz, P.; Komaromi, I.; Martin, R. L.; Fox, D. J.; Keith, T.; Al-Laham, M. A.; Peng, C. Y.; Nanayakkara, A.; Challacombe, M.; Gill, P. M. W.; Johnson, B.; Chen, W.; Wong, M. W.; Gonzalez, C.; Pople, J. A. *Gaussian 03*, revision C.02; Gaussian, Inc.: Wallingford, CT, 2004.
(32) Dunning, T. H., Jr.; Hay, P. J. In *Modern Theoretical Chemistry*; Schaefer, H. F., III, Ed.; Plenum: New York, 1976; Vol. 3, pp 1−28.
(33) Hay, P. J.; Wadt, W. R. *J. Chem. Phys.* **1985**, *82*, 270−283.
(34) Wadt, W. R.; Hay, P. J. *J. Chem. Phys.* **1985**, *82*, 284−298.
(35) Hay, P. J.; Wadt, W. R. *J. Chem. Phys.* **1985**, *82*, 299−310.
(36) Diebler, H.; Secco, F.; Venturini, M. *J. Phys. Chem.* **1987**, *91*, 5106−5111.
(37) Secco, F.; Venturini, M. *J. Chem. Soc., Faraday Trans.* **1993**, *89*, 719−725.
(38) Gonzalez, S. Thesis. University of Burgos: Burgos, Spain, 2005.

Table 1. Equilibrium Constants for the PBHA−Ni(II) and SHA−Ni(II) Systems at 25 °C and $I = 0.2$ M ($NaClO_4$)

ligand	pK_{H_2L}	pK_{HL}	pK_C	$\log K_{MH_2L}$	$\log K_{MHL}$
PHBHA	8.40 ± 0.03[a]	9.40 ± 0.02[a]	5.14 ± 0.02	1.17 ± 0.17	4.44 ± 0.02
				1.23 ± 0.08[b]	4.43 ± 0.08[b]
SHA	7.32 ± 0.04[a]	9.72 ± 0.04[a]	5.19 ± 0.03	2.06 ± 0.22	3.70 ± 0.07
	7.34 ± 0.01[c]	9.77 ± 0.05[c]		0.49 ± 0.21[d]	3.84 ± 0.12[d]

[a] Reference 38. [b] Evaluated as k_1/k_{-1} and k_2/k_{-2}. [c] Values extrapolated to $I = 0.2$ M using an equation which provides the pK_a dependence on the ionic strength for SHA (ref 44). [d] Evaluated as $k_1/k_{-1}(1 + k_3/k_{-3})$ and $k_2/k_{-2}(1+k_4/k_{-4})$, considering that, for SHA, $[MH_2L] = [MH_2L_I] + [MH_2L_{II}]$ and $[MHL] = [MHL_I] + [MHL_{II}]$.

order conditions ($C_M \geq 10C_L$). The acidity level was kept constant during the course of the reaction by using the cacodylic acid/cacodylate ion buffer.

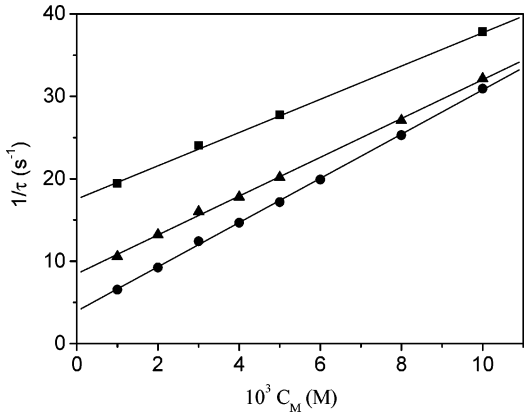

Figure 2. Dependence of the reciprocal relaxation time on the metal ion concentration for the PHBHA−Ni(II) system in an aqueous solution at 25 °C and $I = 0.2$ M. Symbols: squares, $[H^+] = 1.0 \times 10^{-6}$ M; triangles, $[H^+] = 3.9 \times 10^{-7}$ M; circles, $[H^+] = 1.6 \times 10^{-7}$ M.

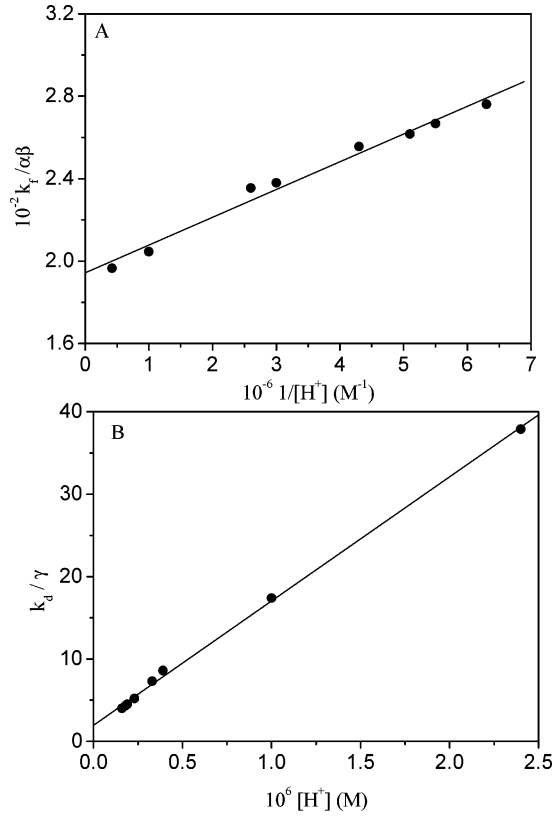

Figure 3. Dependence of the apparent kinetic constants on the medium acidity for the PHBHA−Ni(II) system in an aqueous solution at 25 °C and $I = 0.2$ M: (A) complex formation; (B) complex dissociation.

Table 2. Reaction Parameters for the PHBHA−Ni(II) and SHA−Ni(II) Systems at 25 °C and $I = 0.2$ M ($NaClO_4$)

reaction parameters	PHBHA	SHA
$10^{-3}\, k_1$ ($M^{-1}\, s^{-1}$)	1.9 ± 0.1	2.6 ± 0.1
$10^{-2}\, k_{-1}$ (s^{-1})	1.1 ± 0.1	13 ± 1
$10^{-3}\, k_2$ ($M^{-1}\, s^{-1}$)	32 ± 2	5.4 ± 0.2
k_{-2} (s^{-1})	1.2 ± 0.2	6.3 ± 0.5
k_3 (s^{-1})		3.1 ± 1
k_{-3} (s^{-1})		5.7 ± 0.2
k_4 (s^{-1})		7.8 ± 0.6
k_{-4} (s^{-1})		1.1 ± 0.1
$10^7\, K_{CI}$ (M)		2.4 ± 0.8[a]
$10^7\, K_{CII}$ (M)		6.0 ± 0.9

[a] Average value of the results obtained from eqs 13 and 14.

The PHBHA−Ni^{2+} System. The stopped-flow traces show a single kinetic effect (Figure 3S, Supporting Information). The dependence of the time constant, $1/\tau$, on the metal ion concentration is linear, concurrent with eq 5 (Figure 2). Thus, the slope and intercept of straight lines like those of Figure 2 yielded the forward (k_f) and reverse (k_d) rate constants, respectively, of the apparent reaction 1.

$$1/\tau = k_f C_M + k_d \tag{5}$$

The K_{app} values obtained as k_f/k_d at different $[H^+]$ values are collected in Table 1S (Supporting Information). According to eqs 6 and 7, the apparent rate constants have been found to depend on $[H^+]$

$$k_f/\alpha\beta = k_1 + k_2 K_{H_2L}[H^+]^{-1} \tag{6}$$

$$k_d/\gamma = k_{-2} + k_{-1}K_C^{-1}[H^+] \tag{7}$$

where α and β have been defined above and $\gamma = K_C/([H^+] + K_C)$. The rate constants k_1 and k_{-1} refer to the individual step 3, whereas constants k_2 and k_{-2} refer to step 4 (Scheme 1). The corresponding values were derived from the graphical representation of eqs 6 and 7 (parts A and B of Figure 3) and are collected in Table 2. Bearing in mind that $k_1/k_{-1} = K_{MH_2L}$ and $k_2/k_{-2} = K_{MHL}$, the values of the equilibrium constants of steps 3 and 4 evaluated by the kinetic method ($k_1/k_{-1} = 17\ M^{-1}$ and $k_2/k_{-2} = 2.7 \times 10^4\ M^{-1}$) concur fairly well with those derived from the static measurements ($K_{MH_2L} = 15\ M^{-1}$ and $K_{MHL} = 2.7 \times 10^4\ M^{-1}$).

The SHA−Ni^{2+} System. The SHA−Ni^{2+} system displays two kinetic effects well resolved on the time scale (Figure 4). The binding process could therefore be described by the two-step sequence 8

$$M_f + L_f \underset{k_{dI}}{\overset{k_{fI}}{\rightleftharpoons}} ML_{T,I} \underset{k_{d2}}{\overset{k_{f2}}{\rightleftharpoons}} ML_{T,II} \tag{8}$$

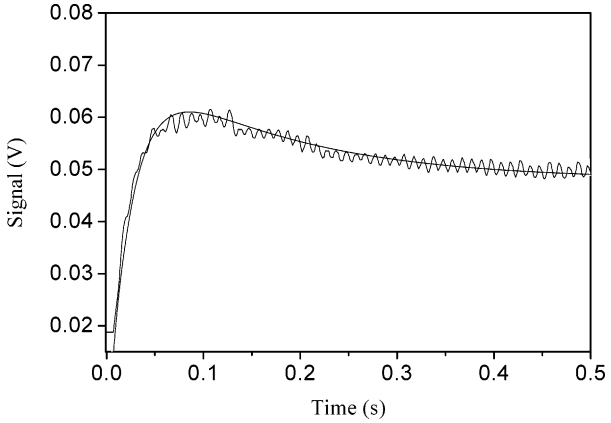

Figure 4. Biexponential kinetic effect observed for the Ni(II)−SHA system. $C_L = 4 \times 10^{-5}$ M, $C_M = 2 \times 10^{-2}$ M, $I = 0.2$ M, $\lambda = 304$ nm, pH = 5.7, 25 °C.

which requires that the time constants of the two effects, $1/\tau_f$ (fast) and $1/\tau_s$ (slow), should depend on the metal ion concentration according to eqs 9 and 10.

$$1/\tau_f = k_{f1}C_M + k_{d1} \quad (9)$$

$$1/\tau_s = (k_{f2}k_{f1}/k_{d1})C_M/(1 + (k_{f1}/k_{d1})C_M) + k_{d2} \quad (10)$$

The values of k_{f1} and k_{d1} are obtained from the analysis, according to eq 9, of the data plotted in Figure 5A, whereas the k_{f2} and k_{d2} values are obtained from the analysis according to eq 10 of the data plotted in Figure 5B. If the reaction sequence 8 is correct, then the apparent equilibrium constant K_{app} should be a function, according to eq 11, of the rate constants of the two processes observed in the kinetic experiments.

$$K_{app} = k_{f1}/k_{d1}(1 + k_{f2}/k_{d2}) \quad (11)$$

The values of K_{app}, obtained as the combination of the rate constants, are collected in Table 2S (Supporting Information). Figure 1 shows the fair agreement between these values and those determined by spectrophotometric titrations at different pH values.

The observed dependence of the rate constants on $[H^+]$ suggests that several forms of both the ligand and the complex, protonated to different extents, should be involved in the binding process. The behavior of the system was further rationalized after rewriting the compact representation of the reacting process (eq 8) in the more detailed form depicted in Scheme 2.

The rate constants k_1 and k_2 are evaluated by the analysis of the data in Figure 6A according to eq 12

Scheme 2

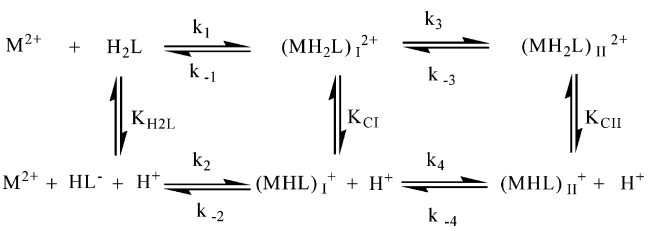

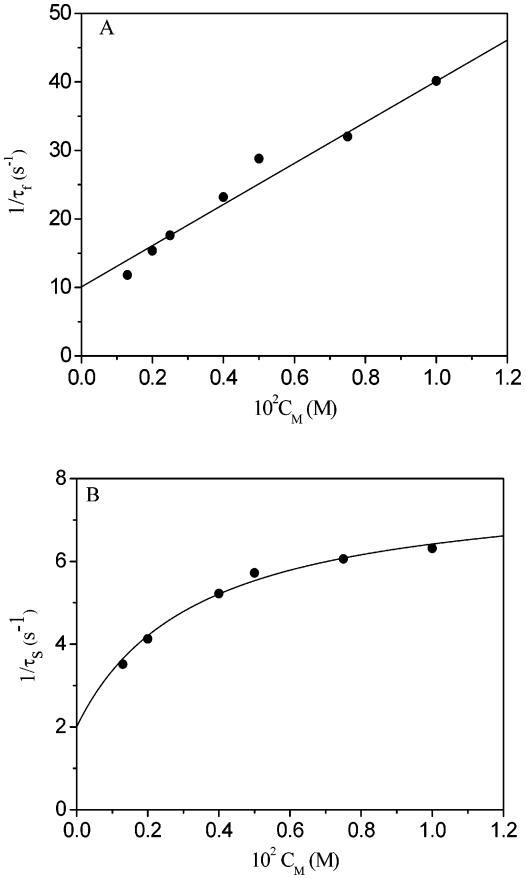

Figure 5. Metal-concentration dependence of the time constants of the two kinetic effects observed for the Ni(II)−SHA system at 25 °C, pH = 6.70 and $I = 0.2$ M: (A) fast effect; (B) slow effect.

$$k_{f1}/\alpha\beta = k_1 + k_2K_{H_2L}/[H^+] \quad (12)$$

whereas k_{-1}, k_{-2}, and K_{CI} are evaluated from data of Figure 6B according to eq 13

$$k_{d1} = (k_{-2} + k_{-1}K_{CI}^{-1}[H^+])\gamma_I \quad (13)$$

where $\gamma_I = K_{CI}/(K_{CI} + [H^+])$. The values of k_3, k_4, and K_{CI} are obtained according to eq 14 (Figure 7A)

$$k_{f2} = (k_3 + k_4K_{CI}/[H^+])(1 - \gamma_1) \quad (14)$$

whereas values of k_{-4}, k_{-3}, and K_{CII} are evaluated according to eq 15 (Figure 7B)

$$k_{d2} = (k_{-4} + k_{-3}K_{CII}^{-1}[H^+])\gamma_{II} \quad (15)$$

where $\gamma_{II} = K_{CII}/(K_{CII} + [H^+])$. The values of the reaction parameters are collected in Table 2.

The SHA−Zn^{2+} System. Figure 4S (Supporting Information) shows a stopped-flow curve obtained by reaction of SHA with $Zn(ClO_4)_2$. The observed single-exponential effect corresponds to the slower of the two effects displayed by the SHA−Ni^{2+} system; in light of the high lability of the Zn^{2+} ion, the first effect was too fast to be observed by the stopped-flow technique.[39] The $1/\tau$ values are independent

(39) Burgess, J. In *Metal Ions in Solution*; Ellis Horwood, Ltd.; Chichester, U.K., 1978.

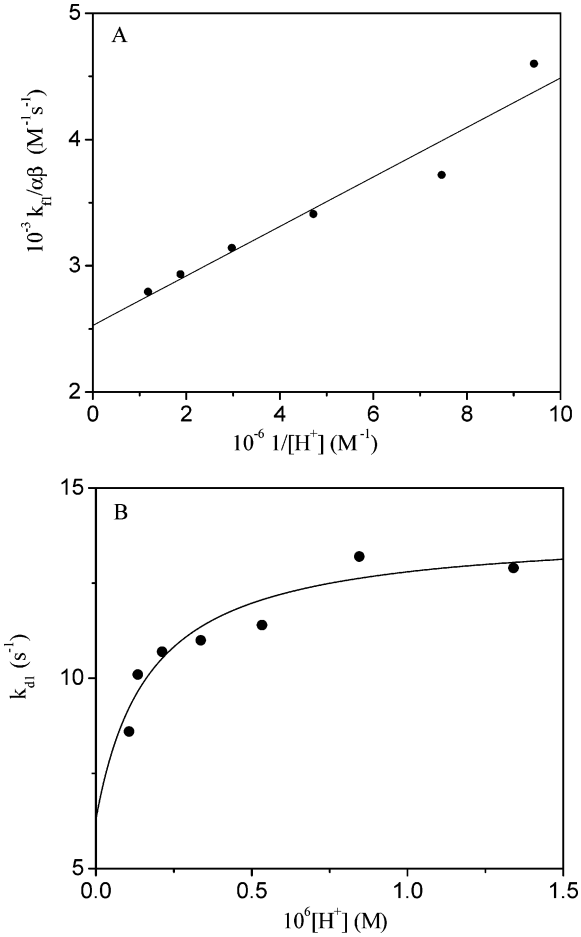

Figure 6. Acidity dependence of the rate constants measured for the fast effect in the Ni(II)−SHA system at 25 °C and $I = 0.2$ M: (A) $M_f + L_f \rightarrow ML_{T,I}$; (B) $ML_{T,I} \rightarrow M_f + L_f$.

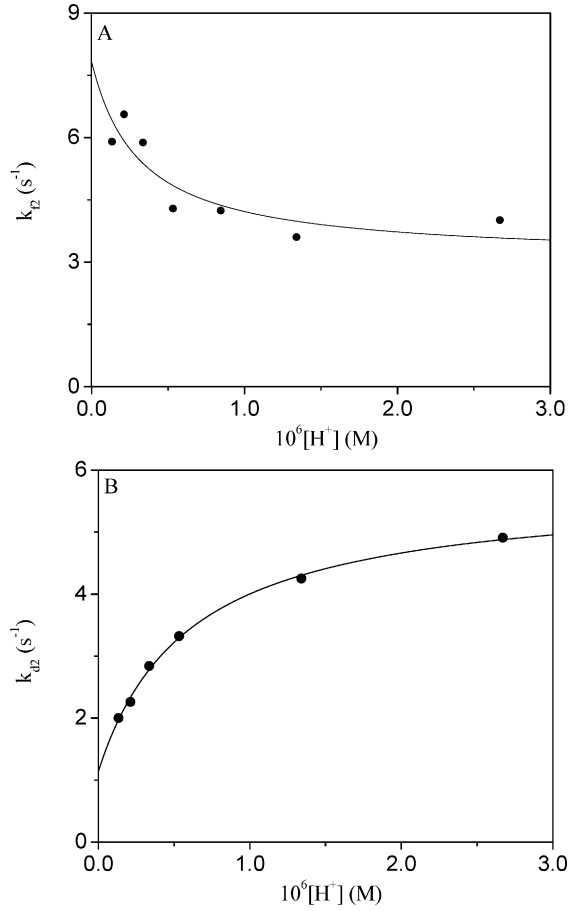

Figure 7. Acidity dependence of the rate constants measured for the slow effect in the Ni(II)−SHA system at 25 °C and $I = 0.2$ M: (A) $ML_{T,I} \rightarrow ML_{T,II}$; (B) $ML_{T,II} \rightarrow ML_{T,I}$.

of the Zn^{2+}concentration, which varied from 1×10^{-3} to 1×10^{-2} M, the average value being 4.2 s^{-1}.

Theoretical Calculations. Table 3 shows the relative energies and the dipole moments of the A and B forms of the Ni(II)−SHA complex and of the Ni(II)−PHBHA complex. The structures of the three complexes are shown in Figure 8. Contrary to the behavior of the free ligand, where the A form was found to be more stable than the B form[19] by 5.3 kcal mol^{-1}, for the Ni(II)−SHA complex the B form turned out to be more stable than the A form by 6.7 kcal mol^{-1}. Comparison of the dipole moment values shows that charge separation is less important in the B chelate. From this point forward, O_P, O_C, and O_H stand for the phenol, carbonyl, and hydroxamic oxygen atoms of the ligands, respectively. It should be noticed that evidence for the presence of the $O_P\cdots H\cdots N$ hydrogen bond in the B form of free SHA has been obtained by ab initio calculations in an argon matrix.[19] The energies of the $Ni(H_2O)_2SHA^+$ (A) and $Ni(H_2O)_2PHBHA^+$ complexes are similar. This means that the $O_P\cdots H\cdots O_C$ hydrogen bond, which stabilizes the A conformation of free SHA, is not present anymore in the $Ni(H_2O)_2SHA^+$ (A) complex. On the other hand, the $O_P\cdots H\cdots N$ hydrogen bond could play an important role in the stabilization of the $Ni(H_2O)_2SHA^+$ (B) conformer.

Table 3. Relative Energies and Dipole Moments of the Investigated Complexes, Calculated with the HF/LanL2DZ (a) and B3LYP/LanL2DZ (b) Methods in the Gas Phase

	relative energy (kcal/mol)		dipole moment (D)	
	a	b	a	b
$Ni(H_2O)_2SHA^+$ (A)	7.20	6.69	18.70	16.79
$Ni(H_2O)_2SHA^+$ (B)	0.0	0.0	15.24	13.54
$Ni(H_2O)_2PHBHA^+$	6.19	6.53	17.99	15.44

Discussion

Equilibria. The linear trend displayed by plots like that of Figure 2S (Supporting Information) demonstrates that, under the experimental conditions ($C_M \gg C_L$), only complexes of molar ratio 1:1 are formed, according to reaction 1. If this behavior is expected for PHBHA, that of SHA deserves some comment, since the SHA−Ni(II) system is known to form metallacrowns, although in nonaqueous solvents. The architecture of metallacrowns is such that a structure like that depicted in Scheme 3 should be involved as an intermediate to macrocycle formation.

This structure could grow by binding a second SHA molecule, and a dimer has indeed been crystallized from methanol containing the SHA and Ni^{2+} ions.[40] The binuclear species, if formed in noticeable amounts in the presently

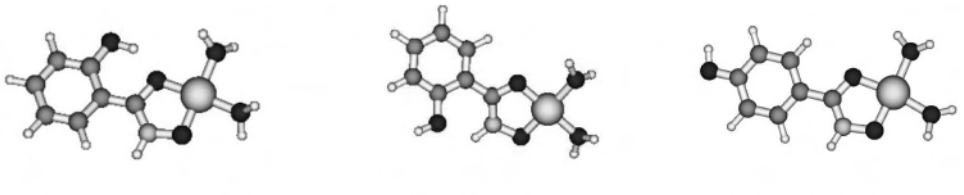

Figure 8. Optimized geometries of the complexes $Ni(H_2O)_2SHA^+$ (A), $Ni(H_2O)_2SHA^+$ (B), and $Ni(H_2O)_2PHBHA^+$.

Scheme 3

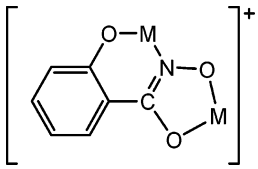

investigated system, would induce deviations from linearity in the trend of Figure 2S (Supporting Information). Moreover, since the binding of two Ni^{2+} ions to a SHA molecule would remove three protons, a dependence of K_{app} on $[H^+]$ different from that shown in Figure 1 would be observed. The kinetic behavior confirms the results of the static experiments.

The complex formation constants of the PHBHA−Ni^{2+}- and SHA−Ni^{2+} systems do not display significant differences. This feature suggests that the phenol group is not involved in the metal binding to SHA and that in the complex is far from the metal center; that is, the SHA−Ni(II) complex has the B conformation, in agreement with the ab initio calculations.

Kinetics. The kinetic behavior of the two systems will be discussed in terms of the I_d mechanism, which characterizes complex formation at Ni(II). According to the Eigen−Tamm argument,[41] $k = k_{H_2O}K_{OS}$, where $k_{H_2O} = 3 \times 10^4\ s^{-1}$ is the rate constant[39] for the water exchange at $Ni(H_2O)_6^{2+}$ and K_{OS} is the stability constant of the outer-sphere complex,[42] whose formation precedes the water−ligand interconversion step.

Concerning the first step of the complex formation, Table 2 shows that the k_1 values corresponding to Ni^{2+} binding to the neutral ligands are close to the k_1 value measured for the Ni^{2+}−BHA system[43] ($k_1 = 1.97 \times 10^3\ M^{-1}\ s^{-1}$). Even with consideration of the reduced electrostatic interaction involved in the binding process ($K_{OS} = (1.5-3) \times 10^{-1}\ M^{-1}$) for a reaction between ions and neutral molecules, the k_1 values remain below the value of the $k_{H_2O}K_{OS}$ product. As for the Ni^{2+}−BHA system, the observed reduction in the reaction rate of Ni^{2+} with the neutral PHBHA and SHA can be put down to an additional energy barrier brought about by the $O_C\cdots H\cdots O_H$ hydrogen bond present at the reaction site. The k_{-1} value for the SHA−Ni(II) system exceeds that of the PHBHA−Ni(II) system by about an order of magnitude. If one takes for granted that the formation of the first metal−ligand bond involves the O_C oxygen, then the faster metal dissociation observed for SHA can be explained by assuming that the O_C−M bond becomes weakened by the hydrogen bond interaction of O_C with the O_PH group.

Concerning the reaction of Ni^{2+} with the HL^- anions of PHBHA and SHA, the k_2 value for the $PHBHA^-$−Ni^{2+} system is perfectly in line with the Eigen−Tamm argument. Actually, for a charge product of 2− and a reaction distance of 5 Å, it turns out that $K_{OS} = 1.6\ M^{-1}$ for $I = 0.2$ M. Consequently, $k_2/K_{OS} = 2.0 \times 10^4\ s^{-1}$, in excellent agreement with the value of k_{H_2O} ($3 \times 10^4\ s^{-1}$). The somewhat lower value of k_2 obtained for the Ni^{2+}−SHA system could be put down to a reduction of the K_{OS} value brought about by the decreased negative density of charge at the O_C site, due to hydrogen bonding with the O_PH group.

The most remarkable difference found in the kinetic behavior of the two systems is given by the slow step, which was observed only with SHA. This finding is explained if one assumes that formation of the O_C−M bond induces the disruption of the $O_P\cdots H\cdots O_C$ hydrogen bond and the subsequent phenol rotation around the C−C bond. Therefore, the resulting chelate will adopt the B conformation. It is reasonable to assume that the B form of the complex is more stable than the corresponding A form, since the positive charge density introduced by the metal ion will push the O_PH group away from the O_C oxygen. This idea has been borne out by the theoretical calculations, which reveal that the B chelate is more stable than the A chelate (Table 3).

Also, it should be noted that the lifetime (ca. 0.3 s) for the observed monomolecular process is too long in comparison with rotations about the C−C bonds. However, the experimental observation could be justified if one assumes that each of the two complexes $MH_2L_I^{2+}$ and MHL_I^+ will distribute between a "closed" and an "open" form in equilibrium, the population of the latter being, by far, in the minority. In this open form, the $O_P\cdots H\cdots O_C$ bond has been broken; therefore, rotation around the C−C bond can occur freely. For instance, let us consider the step associated to k_3, denoting K_3' as the equilibrium ratio [open form]/[closed form] and k_3' as the high rate constant of the phenol rotation around the C−C bond; then, the experimental rate constant is expressed by the relationship $k_3 = K_3'k_3'$. In view that the open form is the minority one, the rotation rate constant will be reduced by a factor equal to K_3'.

A second interpretation could be advanced as well: in SHA, the limiting "quinonelike" form is possible, this being stabilized by the $O_P\cdots H\cdots O_C$ hydrogen bond. As Ni^{2+} ion binds to the O_C atom, the hydrogen bond is weakened and slow

(40) Stemmler, A. J.; Kampf, J. W.; Kirk, M. L.; Pecoraro, V. L. *J. Am. Chem. Soc.* **1995**, *117*, 6368−6369.
(41) Eigen, M.; Tamm, K. *Z. Electrochem.* **1962**, *66*, 107−121.
(42) Fuoss, R. M. *J. Am. Chem. Soc*. **1959**, *80*, 5059−5061.
(43) García, B.; Ibeas, S.; Leal, J. M.; Secco, F.; Venturini, M.; Senent, M. L.; Niño, A.; Muñoz, C. *Inorg. Chem.* **2005**, *44*, 2908−2919.
(44) Ciavatta, L.; De Tommaso, G.; Juliano, M. *Ann. Chim. (Rome, Italy)* **2004**, *94*, 295−302.

rotation around the C═C bond of the "quinonelike" form can occur. However, we prefer the first interpretation since, at room temperature, the rotation process should be faster than that we have measured, as suggested by the NMR measurements carried out on BHA.[43] These measurements show that in BHA the rotation around the C−N bond, which displays a considerable double-bond character, appears to be much faster.

The A → B conversion in the metal complex is expected to be only scarcely affected by the nature of the metal, and actually, the relaxation time of the process does not display a significant variation when Ni^{2+} is replaced by Zn^{2+}. Of course, in the case of Zn^{2+}, the first step is too fast to be observed with the stopped-flow technique, this ion being 1000-fold more labile than Ni^{2+}.[39] For this reason, Figure 4S of the Supporting Information shows only the slow effect.

Acknowledgment. The financial support of Ministerio de Educaciòn y Ciencia, Project CTQ 2006-14734/BQU, and Junta de Castilla y León, Project BU001A-06, is gratefully acknowledged. The authors also acknowledge CESGA (Centro de Supercomputación de Galicia) for the use of their computing facilities.

Supporting Information Available: Apparent equilibrium constants for the PHBHA (Table 1S) and SHA (Table 2S) Ni(II) complexes and the respective spectral changes (Figure 1S), analysis of equilibria for Ni(II)−SHA (Figure 2S), and kinetic effects for Ni(II)−PHBHA (Figure 3S) and Zn(II)−SHA (Figure 4S). This material is available free of charge via the Internet at http// pubs.acs.org.

IC0614061